Brazilian Journal of Physics
ISSN: 0103-9733
luizno.bjp@gmail.com
Sociedade Brasileira de Física
Brasil

Carvalho-Santos, Vagson L.; Dandoloff, Rossen

Topological Spin Excitations Induced by an External Magnetic Field Coupled to a Surface with Rotational Symmetry

Brazilian Journal of Physics, vol. 43, núm. 3, junio, 2013, pp. 130-136
Sociedade Brasileira de Física
São Paulo, Brasil

Braz J Phys (2013) 43:130–136
DOI 10.1007/s13538-013-0126-1

CONDENSED MATTER

Topological Spin Excitations Induced by an External Magnetic Field Coupled to a Surface with Rotational Symmetry

Vagson L. Carvalho-Santos · Rossen Dandoloff

Received: 27 December 2012 / Published online: 10 April 2013

Abstract We study the Heisenberg model in an external magnetic field on curved surfaces with rotational symmetry. The Euler–Lagrange static equations, derived from the Hamiltonian, lead to the inhomogeneous double sine-Gordon equation. Nonetheless, if the magnetic field is coupled to the metric elements of the surface, and consequently to its curvature, the homogeneous double sine-Gordon equation emerges and a 2π-soliton solution is obtained. In order to satisfy the self-dual equations, surface deformations are predicted to appear at the sector where the spin direction is opposite to the magnetic field. On the basis of the model, we find the characteristic length of the 2π-soliton for three specific rotationally symmetric surfaces: the cylinder, the catenoid, and the hyperboloid. On finite surfaces, such as the sphere, torus, and barrels, fractional 2π-solitons are predicted to appear.

Keywords Classical spin models · Solitons · Curvature · Heisenberg Hamiltonian

1 Introduction and Motivation

In the last decades, studies relating the geometry to the physical properties of condensed matter systems (CMS) have attracted much attention. On the one hand, the growing capacity to fabricate and manipulate nanoscale devices with different geometries, examples of which are quasi two-dimensional exotic shapes such as the Möbius strip [1], torus [2–4], and asymmetric nanorings [5], makes it possible to develop and test theoretical models in several branches of CMS, e.g., nanomagnetism, nematic liquid crystals, graphene devices, and topological insulators. On the other hand, theoretical models predict collective modes, which are strongly influenced by the curvature of the substrate. For instance, particle-like excitations, such as vortices and solitons, appear in several contexts in superconductors, ferromagnetic nanoparticles, nematic liquid crystals, Bose–Einstein condensates [6, 7], and colisionless plasmas [8], for example. It has been shown that these particle-like excitations, which have a topological character, interact not only with each other, but also with the curvature of the substrate [9].

In ferromagnetic materials, cylindrical nanomagnets with a vortex as the magnetization ground state have been considered as candidates to be used in logic memory, data storage, highly sensitive sensors [10–13], and cancer therapy [14–16]. Theoretical works have shown that the energy and stability of these topological excitations depend on the curvature of the ferromagnetic nanoparticle [17] and that their dynamical properties are affected both by the interaction with curve defects appearing during fabrication of the nanomagnets [18, 19] and by the magnetic or nonmagnetic impurities present in the magnetic nanoparticles [20].

Vortices can also arise as solutions of the continuous Heisenberg model on two-dimensional systems. In Refs. [21–30], the authors have used this model to analyze the dynamic and static properties of vortices and have shown that the energy of these excitations is closely linked to the characteristic length of the considered geometry. Besides,

V. L. Carvalho-Santos (✉)
Instituto Federal de Educação,
Ciência e Tecnologia Baiano - Campus Senhor do Bonfim,
48970-000 Senhor do Bonfim, Bahia, Brazil
e-mail: vagson.santos@ufv.br

R. Dandoloff
Laboratoire de Physique Théorique et Modélisation,
Université de Cergy-Pontoise,
95302 Cergy-Pontoise, France

the vortex energy presents a divergence in simply connected surfaces, which can be controlled by the development of an out-of-plane component in the vortex core, the so-called vortex polarity. Soliton-like solutions have also been considered in the aforementioned works, and it has been shown that their characteristic lengths depend on the length scale of the surface. For finite surfaces, fractional and half-soliton solutions have been obtained [28, 31].

External fields applied to CMS change the behavior of collective modes and the elastic properties of the systems. For example, an external magnetic field can deform a magnetoelastic metamaterial if a mechanical degree of freedom couples the electromagnetic interaction in the metamaterial lattice to the elastic interaction [32]. In another example, the combination of curvature effects with magnetic fields can reorient the molecular alignment of flux lines of the nematic director of nematic liquid crystals or switch the alignment from one stable configuration to another [33]. In a third illustration, it has been shown that the curvature of graphene bubbles can be controlled by an electric field [34].

In this context, Saxena et al. have considered the exchange and Zeeman terms in the magnetic energy calculations for cylindrical surfaces and shown that the interaction of an external magnetic field with a cylindrical magnetoelastic membrane has a 2π-soliton-like solution, which induces a deformation (pinch) at the sector where the spins and magnetic field point in opposite directions [35, 36]. If a constant magnetic field is applied on an arbitrary curved surface with rotational symmetry, the nonhomogeneuos double sine-Gordon equation (DSG) is obtained, which can only be solved numerically [37, 38]. When the external magnetic field is tuned to the curvature of a surface, however, analytical solutions have been predicted [39].

In this paper, we show that the homogeneous DSG can be obtained for an arbitrary magnetically coated surface with rotational symmetry in the presence of an external magnetic field, provided that the field is tuned to the curvature of the surface. The solution consists of a 2π-soliton, which induces a deformation in the rotationally symmetric surface, due to the magnetic field. In addition, we apply the model to three specific surfaces: the cylinder, catenoid, and hyperboloid, in order to obtain the characteristic length of the 2π-soliton for each of them. The coupling between the magnetic field and the geometry of condensed matter systems is an interesting result, which we believe may guide future work in the control and manipulation of the morphological and physical properties of magnetoelastic coated surfaces, superfluid helium, nematic liquid crystals, graphene bubbles, and topological insulators, since the results in this paper show that magnetoelastic surfaces may be deformed at a specific point by a magnetic field varying from a maximum value, when the radial distance $\rho = 0$, to 0 when $\rho \to \infty$.

This paper is divided as follows: in Section 2, we present our model; the results and discussions are presented in Section 3. Section 4 applies the model to three specific surfaces, and Section 5 presents conclusions and prospects.

2 The Model

The energy of a deformable, magnetoelastically coupled manifold is $E = E_{\text{mag}} + E_{\text{el}} + E_{\text{m-el}}$, where E_{mag}, E_{el}, and $E_{\text{m-el}}$ are the magnetic, elastic, and magnetoelastic contributions to the total energy, respectively. The magnetic contribution is constituted by the exchange, magnetostatic, anisotropy, and Zeeman terms. To describe the magnetic properties of curved surfaces with rotational symmetry under external magnetic fields, we will focus our attention mainly on the exchange and Zeeman contributions. In this case, the energy is well represented by the nonlinear σ-model (NLσM) on a surface in an external magnetic field:

$$H = \iint (\nabla \mathbf{m})^2 dS - g\mu \iint \mathbf{m} \cdot \mathbf{B} dS, \tag{1}$$

where $\mathbf{m}$ is the magnetization unit vector ($\mathbf{m}^2 = 1$), dS is the surface element, $\mathbf{B}$ is the applied magnetic field, μ is the magnetic moment, and g is the gyromagnetic ratio of the electrons in the magnetic material.

This model has been previously used to study the properties of a circular cylinder surface in the presence of a constant axial magnetic field, the well-known DSG [41, 42] having been derived from the Euler–Lagrange equations [35, 36]. The authors obtained a 2π-soliton-like solution and showed that geometrical frustration arises, due to a second length scale introduced by the magnetic field. A surface deformation was predicted at the sector where the spin orientation is opposite to the magnetic field. Whenever applied to arbitrary curved surfaces other than the cylinder, the model has yielded the nonhomogeneous DSG, which could only be solved numerically [37, 38]. Here, we show that the homogeneous DSG system results for any rotationally symmetric surface, if the magnetic field is pointing along the z-axis and its magnitude is a function of the radial distance ρ matched to the curvature of the substrate, that is, $\mathbf{B} \equiv B(\rho)\mathbf{z}$, where $\rho \equiv \rho(z)$ is the distance from a point on the surface to the z-axis.

To proceed with our analysis, it proves convenient to rewrite Eq. (1) on a general geometry with metric tensor g_{ij} and rotational symmetry, described in a cylindrical-like coordinate system. We then have that $g_{\rho\phi} = g_{\phi\rho} = 0$ and the Hamiltonian (1) takes the form

$$H = \iint \sqrt{\frac{1}{g^{\rho\rho} g^{\phi\phi}}} \Big[g^{\rho\rho} (\partial_\rho \Theta)^2 + g^{\phi\phi} \sin^2 \Theta (\partial_\phi \Phi)^2 + g\mu B(\rho)(1 - \cos \Theta) \Big] d\rho d\phi, \tag{2}$$

where $g^{\rho\rho}$ and $g^{\phi\phi}$ are the contravariant metric elements.

The magnetization unit vector is parametrized as $\mathbf{m} = (\sin \Theta \cos \Phi, \sin \Theta \sin \Phi, \cos \Theta)$ and the rotationally symmetric curved surfaces are parametrized in the cylindrical coordinates (ρ, ϕ, z). Cylindrical symmetry is also assumed for the order parameter, that is, $\Theta(\rho, \phi) \equiv \Theta(\rho)$ and $\Phi(\rho, \phi) = \Phi(\phi)$. Since the magnetic field points in the z-axis direction, the Zeeman interaction energy is minimum for $\Theta = 0$ and maximum for $\Theta = \pi$. As discussed below, the surface then undergoes deformation, to minimize the total energy of the system, at the sector of the 2π-soliton where the spins point in the direction opposite to the magnetic field.

3 Results and Discussions

We are interested in static solutions for Heisenberg spins on curved surfaces under external magnetic fields. The Hamiltonian of this system coincides with its Lagrangian $L \equiv L[\Theta, \Phi, \dot{\Theta}, \dot{\Phi}, t]$, that is, $H = L$. To obtain the ground and excited states, we must solve the Euler–Lagrange equations (ELE) for the Hamiltonian (2). The ELE yield the equalities

$$\sqrt{\frac{g^{\rho\rho}}{g^{\phi\phi}}} \partial_\rho \left(\sqrt{\frac{g^{\rho\rho}}{g^{\phi\phi}}} \partial_\rho \Theta \right) = \frac{(\partial_\phi \Phi)^2}{2} \sin 2\Theta + \frac{1}{g^{\phi\phi}} B'(\rho) \sin\Theta \tag{3}$$

and

$$\sin^2 \Theta\, \partial_\phi \left[\sqrt{\frac{g^{\phi\phi}}{g^{\rho\rho}}} \partial_\phi \Phi \right] = 0, \tag{4}$$

where $B'(\rho) \equiv g\mu B(\rho)$.

Since we are considering surfaces with rotational symmetry, the parametric equations associated with Eqs. (3) and (4) can be written in cylindrical-like coordinates with $\mathbf{r} = (\rho \cos \phi, \rho \sin \phi, z(\rho))$, where ρ is the radius of the surface at height z and ϕ denotes the azimuthal angle. In this case, the covariant metric elements are given by the equations

$$g_{\phi\phi} = \frac{1}{g^{\phi\phi}} = \rho^2 \qquad \text{and} \qquad g_{\rho\rho} = \frac{1}{g^{\rho\rho}} = z'^2 + 1, \tag{5}$$

where $z' = \partial z / \partial \rho$. From the above equations, it is easy to see that $\partial_\phi \left(\sqrt{g^{\phi\phi}/g^{\rho\rho}} \right) = 0$ and that Eq. (4) reduces to

$$\sin^2 \Theta \partial_\phi^2 \Phi = 0. \tag{6}$$

Equation (6) admits two kinds of solution. The first kind is defined by the condition $\Theta = n\pi$ ($n = 0, 1, 2, ...$). For even n, the energy associated with the Zeeman term in the Hamiltonian (11) is minimized, while for odd n it is maximized. The odd n solutions, with the spins pointing in the direction opposite to the magnetic field, are unstable. Therefore, the solutions $\Theta = (2n)\pi$ constitute the ground state of the Hamiltonian (1). We are nonetheless interested in excited states, the so-called 2π-solitons, which provide a continuous transition between the two vacua at $\Theta = 0$ and $\Theta = 2\pi$. This class of solutions has been already obtained for the cylinder surface [35, 36], and analytical solutions have been found for other geometries, provided that the magnetic field is coupled to the curvature of the substrate [39]. Here, the simplest way to obtain topological 2π-soliton-like solutions is to consider the next simplest solution of Eq. (6), that is,

$$\Phi(\phi) = \phi + \phi_0 \tag{7}$$

where ϕ_0 is an integration constant with no influence upon the energy calculations.

We can then rewrite Eq. (3) in the form

$$\partial_\xi^2 \Theta = \frac{\sin 2\Theta}{2} + g_{\phi\phi} B'(\rho) \sin \Theta, \tag{8}$$

where $d\xi = \sqrt{g^{\phi\phi}/g^{\rho\rho}} d\rho$.

Two interesting cases can now be identified. In the first case, with $B(\rho) = 0$, Eq. (8) is reduced to the single sine-Gordon equation, and a topological soliton, which satisfies the self-dual equations, is obtained [24, 25]. This particular choice for $B(\rho)$ leads to the isotropic Heisenberg Hamiltonian, which has been previously studied on several curved geometries, e.g., torus [21], cylinder [24–26], sphere [27], pseudosphere [28], cone [29, 30], catenoid, and hyperboloid [37, 38, 40]. The soliton usually has a characteristic length scale (CLS) that depends on the geometrical properties of the underlying manifold. In general, the CLS appears in a factor multiplying the $\sin(2\Theta)$ term on the right-hand side of Eq. (8). This CLS is given by the ratio $\sqrt{g^{\phi\phi}/g^{\rho\rho}}$, which is here embedded in the ξ parameter, so that the CLS of the soliton is rescaled to unity. For the cylinder, for instance, the CLS of the soliton is the constant surface radius ρ_0, any dependence on which can be eliminated by the change of variables $z \to z/\rho_0$ [24, 25].

The second interesting case arises when we consider an arbitrary magnetic field $B(\rho) \neq 0$. If the magnetic field is constant and the arbitrary curved surface has rotational symmetry, Eq. (8) leads to the nonhomogeneous DSG, which calls for numerical treatment [37, 38]. By contrast, if the external field is coupled to the surface curvature by the relation $B'(\rho) = g^{\phi\phi} B'_0$, where $B'_0 = g\mu B(\rho_0)$ and ρ_0 is the surface radius at the $z = 0$ plane, Eq. (8) yields the homogeneous DSG

$$\partial_\xi^2 \Theta = \frac{\sin 2\Theta}{2} + B'_0 \sin\Theta. \tag{9}$$

With $\Theta(-\infty) = 0$ and $\Theta(+\infty) = 2\pi$, the solution of the above equation can be written in the form

$$\Theta(\xi) = 2\tan^{-1}\left(\frac{\rho_B}{\zeta \sinh\frac{\xi}{\zeta}}\right), \tag{10}$$

where $\rho_B^2 = 1/B'_0$ and $\zeta = \rho_B/(1+\rho_B^2)^{1/2}$.

We conclude that the homogeneous DSG is obtained for the Heisenberg spins on curved surfaces in an external magnetic field only if the magnetic field is tuned to the surface curvature, i.e., a function of $1/\rho(z)$.

Equation (10) represents a 2π-soliton, a topological excitation belonging to the second class of the second homotopy group, whose CLS is ζ. As B'_0 grows, the CLS of the soliton shrinks and confines the excitation to progressively smaller regions of the surface. It is also easy to see that $\zeta \to 0$ when $B'_0 \to \infty$. With $B'_0 = 0$, a π-soliton results from Eq. (9), but not from Eq. (10). To understand this finding, we only have to recall that the two solutions belong to two different homotopy classes and cannot be transformed into each other by either continuous transformations or the limiting process $B'_0 \to 0$. The magnetic field introduces a new CLS in the system, which induces geometrical frustration. The CLS of the soliton can no longer be rescaled to unity, and a new CLS arises, given by ζ, which is smaller than the length ρ_B introduced by the magnetic field.

To calculate the energy of the 2π-soliton, we rewrite the Hamiltonian (2) in the form

$$H' = H_1 + H_2 = 2\pi\left[\int_{-\infty}^{\infty}((\partial_\xi\Theta)^2 + \sin^2\Theta)d\xi + \int_{-\infty}^{\infty}\frac{1}{\rho_B^2}(1-\cos\Theta)d\xi\right], \tag{11}$$

where H_1, which corresponds to the first integral within the square brackets on the right-hand side, is independent of the magnetic field and H_2 is the Zeeman term.

We can then compute the soliton energy. The result is

$$E_S = 8\pi\left[\left(1+\frac{1}{\rho_B^2}\right)^{1/2} + \frac{1}{\rho_B^2}\sinh^{-1}\rho_B\right], \tag{12}$$

which is larger than the minimum energy $E_{2\pi S} = 8\pi$ for the homotopy class with winding number $Q = 2$. Only in the limit $\rho_B \to \infty$ do we have $E_S \to 8\pi$ and $\zeta \to 1$. Since $\rho_B = \sqrt{1/B'(\rho_0)}$, the soliton energy depends on the magnitude of the magnetic field at the $z = 0$ plane. The geometrical frustration introduced by the magnetic field will be washed out on elastic surfaces, which will undergo deformation to reduce the radius of the region where the soliton is centered. This will minimize the energy of the two terms independent of the magnetic field in the Hamiltonian (11). Furthermore, if the first term in the development of ELE is considered, one finds that

$$\partial_\xi^2\Theta = \frac{\sin 2\Theta}{2}, \tag{13}$$

as expected.

Equation (13) is the single sine-Gordon equation, whose solution is

$$\Theta = 2\arctan(e^{\xi}). \tag{14}$$

Equation (14), which represents a π-soliton interpolating the two minima, $\Theta = 0$ and $\Theta = \pi$, belongs to the first class of the second homotopy group. As already explained, the π-soliton solution cannot be obtained from the limit $B \to 0$ of Eq. (10), nor do we obtain the π-soliton energy, predicted by the Bogomol′nyi inequality [43], when we set $B = 0$ in Eq. (12).

We will now focus our attention on the last term in Hamiltonian H' (11), which depends on the external magnetic field:

$$H_2 = 2\pi\int_{-\infty}^{\infty}\frac{1}{\rho_B^2}(1-\cos\Theta)d\xi. \tag{15}$$

Substitution of the solution (10) on the right-hand side of Eq. (15) yields the expression

$$H_2 = 4\pi\int_{-\infty}^{\infty}\frac{1}{\rho_B^2}\left[\frac{1}{1+(1-\zeta^2)\sinh^2\frac{\xi}{\zeta}}\right] d\xi = 4\pi\int_{-\infty}^{\infty} f(\rho_B,\xi)d\xi. \tag{16}$$

The energy associated with this part of the Hamiltonian will decrease if we locally decrease ξ while keeping it constant in Eq. (10). Therefore, for a magnetic field tuned to the surface, if the surface cross section is kept at $\xi \pm\infty$, the surface will be deformed in the region of the soliton. For small magnetic fields, we find that

$$E_S = 8\pi\left[1 + \frac{1}{2\rho_B^2}(1+2\ln 2\rho_B)\right] \tag{17}$$

and that $E_S = 8\pi/\rho_B$ for large fields.

As expected, the highest contribution of the external magnetic field to the magnetic energy density comes from the sector where the spin orientation is opposite to the field, which would disappear if the 2π-solitons were to collapse. The resulting alignment of the spins would nonetheless be energetically unfavorable, because the system would then fall in a π-soliton sector of the second homotopy group, which gains infinite energy from the interaction between the spins at $+\infty$ and the magnetic field. We see that the curvature introduces a hard-core repulsion between the two π-solitons in the system. The new CLS associated with the magnetic field introduces geometric frustration, which raises the energy in Eq. (12) above 8π. Surface deformation will then push the magnetic energy down towards the second homotopy class [35, 36] until a balance is reached between the gain in magnetic energy and the loss in elastic energy associated with the surface distortion. We conclude that an elastic membrane coated with a magnetic material will be deformed by an inhomogeneous magnetic field with magnitude adjusted to decay with increasing surface radius ρ.

In the absence of an external field, i.e., with $B_0 = 0$, the self-dual equation of Eq. (9) is $\partial_\xi \Theta = \pm \sin \Theta$. For the DSG, we can write that

$$\partial_\xi \Theta = \pm \sin \Theta \left[1 + \frac{4 \sin^2(\Theta/2)}{\rho_B^2 \sin^2 \Theta} \right]. \tag{18}$$

With the function in square brackets being greater than unity for all $\Theta(\xi)$, the self-dual equation is not satisfied. We conclude that the surface must be deformed to satisfy the self-dual equation and lower the energy. All solutions of Eq. (18) satisfy ELE, but not vice versa. The 2π-soliton lattice of the double sine-Gordon equation in the two regimes $\rho_B \leq 1$ and $\rho_B > 1$ is similar to that on the cylinder [35, 36].

4 Some Specific Cases

On infinite surfaces with rotational symmetry, 2π-soliton solutions are expected, with CLSs that depend on the geometry of the substrate. We will apply our results to rotationally symmetric infinite surfaces to find the soliton CLS associated with each geometry. We will consider the three geometries in Fig. 1: the cylinder, the catenoid, and the hyperboloid. Notwithstanding the similarity between the shapes of the catenoid and hyperboloid surfaces, their geometric properties are different, as we will presently show. The 2π-soliton, given by the solution (10) cannot be found on finite surfaces, such as the sphere, torus, or barrels. In these cases, only fractional solitons can occur, because the spin sphere will not be completely covered twice, as it should be in order to define an excitation in the second class of the second homotopy group. Topological arguments cannot be used, therefore, to ensure the stability of the excitation.

We first analyze the surface of the cylinder, previously studied by Saxena et al. [35, 36]. In that work, the authors have predicted the appearance of a 2π-soliton in a constant magnetic field and found its CLS as a function of z. The cylinder has null Gaussian curvature, and its mean curvature is $M = 1/2r$. Since $z(\rho) \equiv z$ is a constant, the cylindrical coordinate parametrization leads to the metric elements

$$g_{\phi\phi}^{\text{cyl}} = \rho^2 = r^2 \qquad \text{and} \qquad g_{\rho\rho}^{\text{cyl}} = 1, \tag{19}$$

where r is the cylinder radius.

It can be easily seen that a uniform magnetic field $B'(\rho)_{\text{cyl}} = (1/r^2)B'_0$ has to be applied to the surface and that the CLS is

$$\xi_{\text{cyl}} = \ln r. \tag{20}$$

Had we considered z, instead of ρ, as our variable, this result would coincide with Eq. (4) in Refs. [35, 36].

From Eq. (8), we conclude that the homogeneous DSG can be obtained from the Heisenberg model in an external field for any rotationally symmetric surface, not only the cylinder, as long as the magnitudes of the magnetic fields be appropriate functions of the metric element $g_{\phi\phi}$. By contrast, if a uniform magnetic field is applied to an arbitrarily curved magnetoelastic surface, the solutions to the model described by Eq. (1) lead to the inhomogeneous DSG, which must be solved numerically [37, 38]. We will next consider two surfaces with negative, variable Gaussian curvature, namely the catenoid and the hyperboloid.

The catenoid is a minimal surface, its mean curvature being equal to zero everywhere. In contrast with the cylinder surface, however, its Gaussian curvature is nonzero. Indeed, the Gaussian curvature of the catenoid, given by the expression

$$K = -\frac{1}{\rho^2} \text{sech}^4 \left(\frac{z}{\rho} \right), \tag{21}$$

is negative.

Another distinction between the catenoid and the cylinder is the variable radius of the catenoid, the z-dependence of which is given by the expression

$$\rho(z) = r \cosh(z/r). \tag{22}$$

The catenoid can be parametrized by the triad $(\rho \cos \phi, \rho \sin \phi, r \cosh^{-1}(\rho/r))$, where r is the radius of the surface at the $z = 0$ plane. This parametrization leads to the equalities

$$g_{\phi\phi}^{\text{cat}} = \rho^2 \qquad \text{and} \qquad g_{\rho\rho}^{\text{cat}} = \frac{\rho^2}{\rho^2 - r^2}. \tag{23}$$

To yield the homogeneous DSG, the magnetic field $B'(\rho)_{\text{cat}} = (1/\rho^2)B'_0$ has to be applied on this surface. Since ρ is a function of z, as shown by Eq. (22), the magnetic field is nonuniform. In particular, as $\rho \to \infty$, the field tends to zero and, at $\rho(0) = r$, it reaches the maximum $B'(\rho = r)_{\text{cat}} = (1/r^2)B'_0$. It is a simple matter to calculate

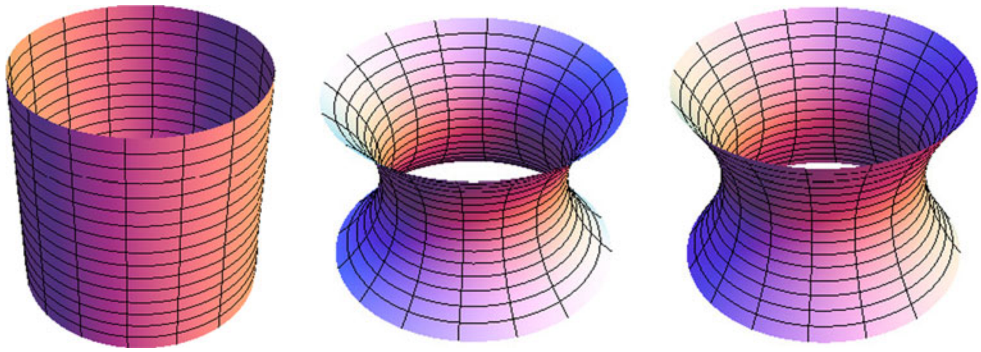

Fig. 1 [Colored online] Surfaces of a cylinder, a catenoid, and a hyperboloid, all of which have rotational symmetry. In each case, to generate a 2π-soliton the magnetic field must be coupled to the curvature. In the case of the cylinder, the magnetic field must be uniform, while the fields for the catenoid and hyperboloid vary with ρ, its magnitude being maximum on the $z = 0$ plane and vanishing as $\rho \to \pm\infty$

the CLS on the catenoid in an external nonuniform magnetic field, which admits a 2π-soliton solution with

$$\xi_{\text{cat}} = \ln\left[2\left(\rho + \sqrt{\rho^2 - r^2}\right)\right]. \tag{24}$$

Finally, we apply our model to the hyperboloid, a shape similar to the catenoid. While the mean curvature of the catenoid is zero everywhere, the hyperboloid has variable mean and Gaussian curvatures [44]. A one-sheeted hyperboloid can be parametrized by the triad $(\rho\cos\phi, \rho\sin\phi, (b/r)\sqrt{\rho^2 - r^2})$, where again r is the radius of the surface at $z = 0$ and b is a multiplicative parameter accounting for the height of the surface. This parametrization leads to the relations

$$g_{\phi\phi}^{\text{hyp}} = \rho^2 \qquad \text{and} \qquad g_{\rho\rho}^{\text{hyp}} = \frac{\rho^2(b^2 + r^2) - r^4}{r^2(\rho^2 - r^2)}. \tag{25}$$

From now on, in order to obtain analytical solutions, we will use the biharmonic coordinate system (BC) with $b = r$ to describe a particular kind of hyperboloid [45], here called the polar hyperboloid. In this case, the equation describing the metric element simplifies to the form

$$g_{\rho\rho}^{\text{phyp}} = \frac{2\rho^2 - r^2}{\rho^2 - r^2}, \tag{26}$$

and to yield the homogeneous DSG, the magnetic field must have the form $B'(\rho)_{\text{hyp}} = (1/\rho^2)B'_0$.

Thus, as in the case of the catenoid, to yield a 2π-soliton, the magnetic field must be ρ dependent, its maximum, at $z = 0$, being given by the equality $B'(\rho = r)_{\text{hyp}} = (1/r^2)B'_0$. One can easily show that the magnetic field applied on the hyperboloid described by BC is a function of $\rho = \sqrt{r^2 + z^2}$, so that $B'(\rho)_{\text{hyp}} \to 0$ as $z(\rho) \to \pm\infty$.

The polar hyperboloid also admits the solution given by Eq. (10). The ξ parameter for this surface is given by an expression too long to be recorded here.

Although $\lim_{\rho\to\infty} B(\rho) = 0$, the total magnetic flux through the catenoid and hyperboloid diverges as $\ln\rho$ as $\rho \to \infty$. Through the cylinder, however, the flux is nonetheless a finite function of the radius r.

5 Conclusions and Prospects

In conclusion, we have shown that the homogeneous DSG is the Euler–Lagrange equations derived from the continuum approach to classical Heisenberg spins on a rotationally symmetric surface under an external magnetic field in the $\hat{z}$-direction, provided that the field is coupled to the curvature of the surface. For arbitrary surface in this model, we have found a single 2π-soliton-like solution. In the sector with spins in the $-\hat{z}$-direction, surface deformations were predicted, which lower the energy to values closer to the bound in Bogomol′nyi inequality.

We have applied this model to three specific surfaces: the cylinder, catenoid, and hyperboloid, which have different geometrical properties, characteristic length scales, and Gaussian curvatures. As expected, each of the three surfaces admits a 2π-soliton, and in each case the magnetic field yielding the homogeneous DSG is a function of $\rho(z)$, but the function depends on the surface. While a uniform field yields the homogeneous DSG on the cylinder, the magnetic fields associated with the homogeneous DSG on the catenoid and hyperboloid are inversely proportional to $\rho(z)$. Since the characteristic length of the soliton depends on the magnitude of the field, the amount of deformation can be controlled by the magnitude of the applied magnetic field. Finite surfaces admit fractional 2π-solitons, which are topologically unstable.

Our results identify experimentally observable magnetoelastic effects. For example, membranes coated with magnetic material can be deformed this way. Additional theoretical work attentive to the surface tension is needed to quantitatively describe the deformation dynamics of magnetically coated membranes and of magnetoelastic metamaterials [32]. We also expect our findings to aid future studies targeting the manipulation and control of morphological and physical properties of nematic liquid crystals, curved graphene sheets, and topological insulators.

Acknowledgments We thank the CNPq (grant number 562867/2010-4) and Propes of the IF Baiano, for financial support. Carvalho-Santos thanks J. D. Lima, P. G. Lima-Santos, and G. H. Lima-Santos for their encouragement.

References

1. S. Tanda, T. Tsuneta, H. Okajima, K. Inagaki, K. Yumaya, N. Hatakenaka, Nature **417**, 397 (2002)
2. E. Yazgan, E. Taşci, O.B. Malcioğlu, Ş. Erkoç, J. Mol. Struct. **681**, 231 (2004)
3. E. Taşci, E. Yazgan, O.B. Malcioğlu, Ş. Erkoç, Fuller. Nanotub. Carbon Nanostruct. **13**(147) (2005)
4. F.-M. Liu, M. Green, J. Mater. Chem. **14**, 1526 (2004)
5. F.Q. Zhu, G.W. Chern, O. Tchernyshyov, X.C. Zhu, J.G. Zhu, C.L. Chien, Phys. Rev. Lett. **96**, 027205 (2006)
6. P.M. Chaikin, T.C. Lubensky, *Principles of Condensed Matter Physics* (Cambridge University Press, Cambridge, 2006). 3rd printing
7. N.D. Mermin, Rev. Mod. Phys. **51**, 591 (1979)
8. M.N.S. Qureshi, J. Shi, H.A. Shah, Bras. J. Phys. **42**, 48 (2012)
9. V. Vitelli, A.M. Turner, Phys. Rev. Lett. **93**, 215–301 (2004)
10. J. Dai, J.-Q. Wang, C. Sangregorio, J. Fang, E. Carpenter, J. Tang, J. Appl. Phys. **87**, 7397 (2000)
11. G.A. Prinz, J. Magn. Magn. Mater. **200**, 57 (1999)
12. S.H. Sun, C.B. Murray, D. Weller, L. Folks, A. Moser, Science **287**, 1989 (2000)
13. G.A. Prinz, ibid. **282**, 1660 (1998)
14. D.-H. Kim, E. Rozhkova, I. Ulasov, S. Bader, T. Rajh, M. Lesniak, V. Novosad, Nat. Matter (2009). doi:10.1038/NMAT2591
15. E.A. Rozhkova, V. Novosad, D.-H. Kim, J. Pearson, R. Divan, T. Rajh, S.D. Bader, J. Appl. Phys. **105**, 07B306 (2009)
16. E.A. Rozhkova, I. Ulasov, B. Lai, N.M. Dimitrijevic, M.S. Lesniac, T. Rajh, Nano Lett. **9**, 3337 (2009)
17. V.L. Carvalho-Santos, W.A. Moura-Melo, A.R. Pereira, J. Appl. Phys. **108**, 094310 (2010)
18. F.A. Apolonio, W.A. Moura-Melo, F.P. Crisafuli, A.R. Pereira, R.L. Silva, J. Appl. Phys. **106**, 084320 (2009)
19. A. Vansteenkiste, M. Weigand, M. Curcic, H. Stoll, G. Schütz, B. Van Waeyenberge, New J. Phys. **11**, 063006 (2009)
20. D. Toscano, S.A. Leonel, R.A. Dias, P.Z. Coura, B.V. Costa, J. Appl. Phys. **109**, 076104 (2011)
21. V.L. Carvalho-Santos, A.R. Moura, W.A. Moura-Melo, A.R. Pereira, Phys. Rev. **B77**, 134450 (2008)
22. J. Benoit, R. Dandoloff, Phys. Lett. **A248**, 439 (1998)
23. A. Saxena, R. Dandoloff, T. Lookman, Physica **A261**, 13 (1998)
24. R. Dandoloff, S. Villain-Guillot, A. Saxena, A.R. Bishop, Phys. Rev. Lett. **74**, 813 (1995)
25. S. Villain-Guillot, R. Dandoloff, A. Saxena, A.R. Bishop, Phys. Rev. **B52**, 6712 (1995)
26. L.A.N. de Paula, Bras. J. Phys. **39**, 711 (2009)
27. G.S. Milagre, W.A. Moura-Melo, Phys. Lett. **A368**, 155 (2007)
28. L.R.A. Belo, N.M. Oliveira-Neto, W.A. Moura-Melo, A.R. Pereira, E. Ercolessi, Phys. Lett. **A365**, 463 (2007)
29. W.A. Freitas, W.A. Moura-Melo, A.R. Pereira, Phys. Lett. **A336**, 412 (2005)
30. W.A. Moura-Melo, A.R. Pereira, L.A.S. Mól, A.S.T. Pires, Phys. Lett. **A360**, 472 (2007)
31. A. Saxena, R. Dandoloff, Phys. Rev. **B66**, 104414 (2002)
32. M. Lapine, I.V. Shadrivov, D.A. Powell, Y.S. Kivshar, Nat. Mater. **11**, 30 (2012)
33. G. Napoli, L. Vergori, Phys. Rev. Lett. **108**, 207803 (2012)
34. T. Georgiou, L. Britnell, P. Blake, R.V. Gorbachev, A. Gholinia, A.K. Geim, C. Casiraghi, K.S. Novoselov, Appl. Phys. Lett. **99**, 093103 (2011)
35. A. Saxena, R. Dandoloff, Phys. Rev. **B58**, R563 (1998)
36. R. Dandoloff, A. Saxena, Eur. Phys. J. **B29**, 265 (2002)
37. A. Saxena, R. Dandoloff, Phys. Rev. **B66**, 104414 (2002)
38. R. Dandoloff, A. Saxena, J. Phys. A Math. Theor. **44**, 045203 (2011)
39. V.L. Carvalho-Santos, R. Dandoloff, Phys. Lett. **A376**, 3551 (2012)
40. V.L. Carvalho-Santos, R. Dandoloff, On geometry-dependent vortex stability and topological spin excitations on curved surfaces with cylindrical symmetry. Phys. Lett. A (2013). doi:10.1016/j.physleta.2013.03.028
41. K.M. Leung, Phys. Rev. **B26**, 226 (1982)
42. K.M. Leung, Phys. Rev. **B27**, 2877 (1983)
43. E.B. Bogomolnyi, Sov. J. Nucl. Phys. **26**, 449 (1976)
44. E.W. Weisstein, Hyperboloid. (MathWorld—A Wolfram Web Resource, 2013). http://mathworld.wolfram.com/Hyperboloid.html. Accessed 30 Nov 2012
45. K. Kowalski, J. Rembieliński, A. Szcześniak, J. Phys. A: Math. Theor. **44**, 085302 (2011)